Microsc. Microanal. 19, S5, 21–24, 2013
doi:10.1017/S1431927613012257

Statistical Analysis on Static Recrystallization Texture Evolution in Cold-Rolled AZ31 Magnesium Alloy Sheet

Jun-Ho Park,[1] Tae-Hong Ahn,[1] Hyun-Sik Choi,[1] Jung-Man Chung,[2] Dong-Ik Kim,[2] Kyu Hwan Oh,[1] and Heung Nam Han[1,*]

[1]*Department of Materials Science and Engineering, Center for Iron and Steel Research, RIAM, Seoul National University, San 56-1, Shinrim-dong, Kwanak-gu, Seoul 151-744, Republic of Korea*
[2]*High Temperature Energy Materials Research Center, Korea Institute of Science and Technology, Hwarangno 14-gil 5, Seongbuk-gu, Seoul 136-791, Republic of Korea*

Abstract: Cast AZ31B-H24 magnesium alloy, comprising Mg with 3.27 wt% Al and 0.96 wt% Zn, was cold rolled and subsequently annealed. Global texture evolutions in the specimens were observed by X-ray diffractometry after the thermomechanical processing. Image-based microstructure and texture for the deformed, recrystallized, and grown grains were observed by electron backscattered diffractometry. Recrystallized grains could be distinguished from deformed ones by analyzing grain orientation spread. Split basal texture of ca. ±10–15° in the rolling direction was observed in the cold-rolled sample. Recrystallized grains had widely spread basal poles at nucleation stage; strong {0001} basal texture developed with grain growth during annealing.

Key words: AZ31, texture, magnesium, EBSD, recrystallization, misorientation, annealing, rolling

Introduction

Magnesium alloys have potential structural applicability as replacements for heavier materials such as steel, on account of their low density and high specific strength (Mordike & Ebert, 2001; Pérez-Prado & Ruano, 2003; Barnett et al., 2004; Easton et al., 2008; Ha et al., 2010; Kang et al., 2010; Lee et al., 2010). However, a critical disadvantage is their poor formability at room temperature, which hinders their formation into complex shapes. The poor cold workability is caused by the shortage of independent slip systems in the hexagonal close-packed structure and the development of {0001} basal texture parallel to the sheet plane normal during rolling and subsequent annealing (Keshavarz & Barnett, 2006; Park & Han, 2010). It has been reported that hot-rolled magnesium alloy sheets have strong {0001} basal texture parallel to the sheet plane normal (Pérez-Prado et al., 2004; Huang et al., 2009). Cold rolling below the recrystallization temperature has been reported to favor the formation of split peaks, which are basal poles inclined toward the rolling direction (RD) ca. ±10–15° from the normal of the sheet plane over the development of strong basal texture (Styczynski et al., 2004; Park & Han, 2010). These differences between the textures of hot- and cold-rolled magnesium alloy sheets are possibly associated with recrystallization and growth of the grains (Étienne et al., 2010).

Therefore, this work reports the relationship between the recrystallization and texture evolution of magnesium alloy sheets during rolling and subsequent heat treatment. Texture evolutions were analyzed by X-ray diffractometry (XRD) and electron backscattered diffractometry (EBSD). Attention was especially paid to the changes of image-based microstructure and texture, from deformed grains to their recrystallization and growth.

© MICROSCOPY SOCIETY OF AMERICA 2013
*Corresponding author. E-mail: hnhan@snu.ac.kr

Experimental

AZ31B-H24 magnesium alloy, comprising Mg with 3.27 wt% Al and 0.96 wt% Zn, was cast, sliced into 4.7 mm sheets for rolling, and then homogenized at 623 K for 24 h. The average grain size determined by optical microscopy was 132 μm. Samples were then multi-pass cold rolled at room temperature with a rolling speed of 1.6 m/min, undergoing up to ca. 37% reduction, the maximum allowable reduction before failure. Lubricating oil was used to minimize friction between the rollers and the sheet. After deformation, the rolled sheets were annealed for varying periods of time at a temperature above the recrystallization temperature (483 K) of AZ31 alloy.

Global texture changes of the specimens during the thermomechanical processing were analyzed by XRD (PANalytical X'Pert PRO). Pole figures were measured by reflection X-ray. An EBSD system (HKL Nordlys, Channel 5) was used for the measurement of image-based microstructure and texture. All measurements were carried out in a scanning electron microscope (JEOL, JSM-6500F) equipped with a field emission gun. Samples were prepared for EBSD measurement by standard metallographic grinding and polishing for 20 min with 0.04 μm colloidal silica. The specimens were then chemically etched for 10 s with a solution of 5 mL nitric acid, 15 mL acetic acid, 20 mL distilled water, and 30 mL ethanol solution.

Results and Discussion

Figures 1a–1d show the {0001} pole figures determined by XRD of the as-rolled sample and samples annealed for 2.5, 50 min, and 18.5 h at 623 K, respectively. The cold-rolled

https://doi.org/10.1017/S1431927613012257 Published online by Cambridge University Press

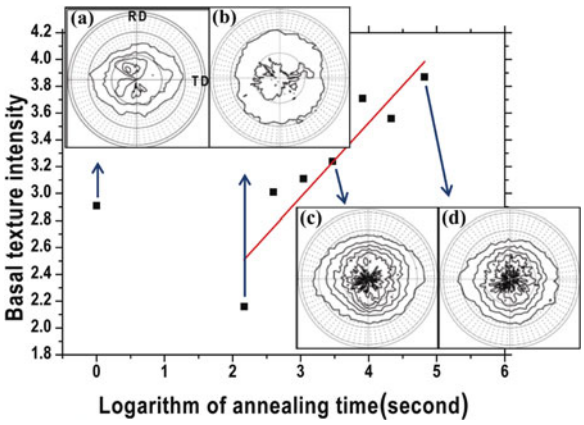

Figure 1. Basal texture intensity with respect to annealing time and {0001} pole figures of samples: (**a**) as-rolled and after (**b**) 2.5 min, (**c**) 50 min, and (**d**) 18.5 h annealing at 623 K.

sample, after 37% reduction, had a texture with basal poles tilted ca. ±10–15° from the normal direction (ND) toward RD, in good agreement with other reports of cold-rolled magnesium alloy sheet that showed splitting of the basal poles in RD (Kim et al., 2002; Chino & Mabuchi, 2009). During early annealing (Fig. 1b), the crystallographic orientations were broadly spread circularly around the basal pole. As the annealing progressed, the basal texture tended to become stronger (Figs. 1c, 1d). Quantitative analysis of basal texture intensity changes with annealing time was achieved by measuring the average intensity of the {0001} poles within 5° of the ND, defined as "basal texture intensity." It can be seen that "basal texture intensity" linearly increases as logarithmic annealing time increases.

To observe directly the image-based microstructure and texture of magnesium alloy sheet as its grains progressed from being deformed through their recrystallization and growth, EBSD measurements of the various samples were taken. Figures 2a and 2b, respectively, show an EBSD orientation map parallel to ND and a corresponding {0001} pole figure for the cold-rolled sample after 37% reduction. A grain identification standard of 5° was used (Field, 1995; Kim et al., 2002). Although only a few grains were captured in the map because of the large initial grain size, split basal texture was observed on the pole figure (Fig. 2b), similar to the XRD data in Figure 1a. Similar texture evolutions were observed across the sample.

Figure 3a shows an EBSD orientation map parallel to the ND for a partially recrystallized sample, which was annealed for 10 min at 653 K. To distinguish recrystallized grains from deformed ones, intra-grain misorientation was quantified by a grain orientation spread (GOS; Kim et al., 2002, 2004). GOS, which represents the mean misorientation of all the pixels in a grain from the mean orientation of the grain, is given by

$$\frac{\sum_i \sum_j \min\left[\cos^{-1}\left\{\frac{tr((\mathbf{P}_{\mathbf{A}}^{\text{average}} \cdot \mathbf{P}_{\mathbf{A:i,j}}^{-1}) \cdot \mathbf{S}) - 1}{2}\right\}\right]}{\mathbf{N_A}}$$

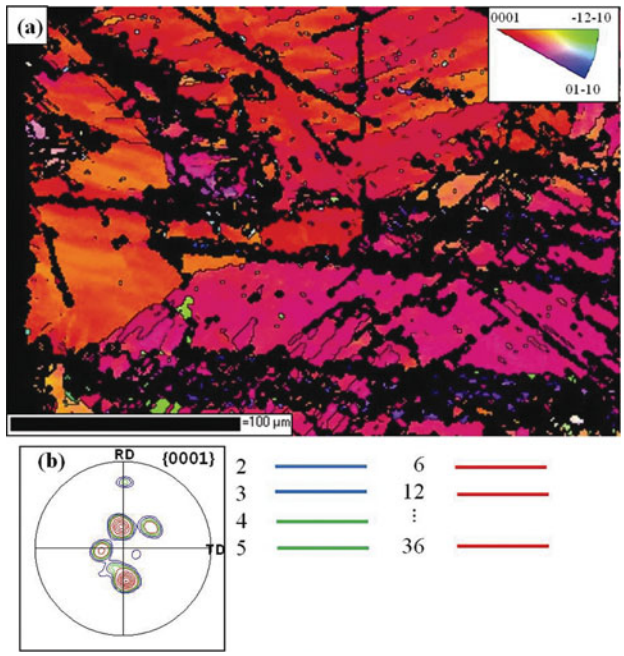

Figure 2. (**a**) Electron backscattered diffractometry orientation map parallel to the normal direction and (**b**) {0001} pole figure of the as-rolled sample.

where $\mathbf{P}_{\mathbf{A}}^{\text{average}}$, $\mathbf{P}_{\mathbf{A:i,j}}$, $\mathbf{N_A}$, and $\mathbf{S}$ are the orientation matrix for the average orientation in grain A, the orientation matrix for a given data point in grain A, the total number of pixels in grain A, and the symmetry group for the given crystal structure, respectively. Here, recrystallized grains could be distinguished from the deformed grains by a critical GOS of 1.5°. Figure 3a shows that the area fraction of ca. 66% was recrystallized. The average grain size and the standard deviation of the recrystallized grains were 7.7 and 3.9 μm, respectively.

Figures 3b–3d show pole figures for overall area, deformed grains (GOS $>$ 1.5°), and recrystallized grains (GOS $<$ 1.5°). Strong split basal texture remained in the deformed grains, indicating that their orientation did not change during annealing, although the recovery might occur. Poles of the recrystallized grains were widely spread around the basal pole (Fig. 3d). Figures 3e–3g show the {0001} pole figures of recrystallized grains with grain sizes $<$3.8 μm (mean grain size minus one positive standard deviation), between 3.8 and 11.6 μm (mean grain size plus one positive standard deviation), and $>$11.6 μm, respectively. The smaller grains showed more widely spaced {0001} poles. The larger grains showed strong basal texture. Smaller grain represented the early stage of annealing, which was dominated by nucleation, whereas the larger grains were indicative of growth subsequent to nucleation. Therefore, these results agree well with the XRD data with annealing times (Fig. 1).

Figure 4a shows the EBSD orientation map parallel to the ND of a sample with grains that had almost completely recrystallized and grown. This sample was annealed for 18 h at 723 K. Using a critical GOS of 1.5°, it was confirmed that

https://doi.org/10.1017/S1431927613012257 Published online by Cambridge University Press

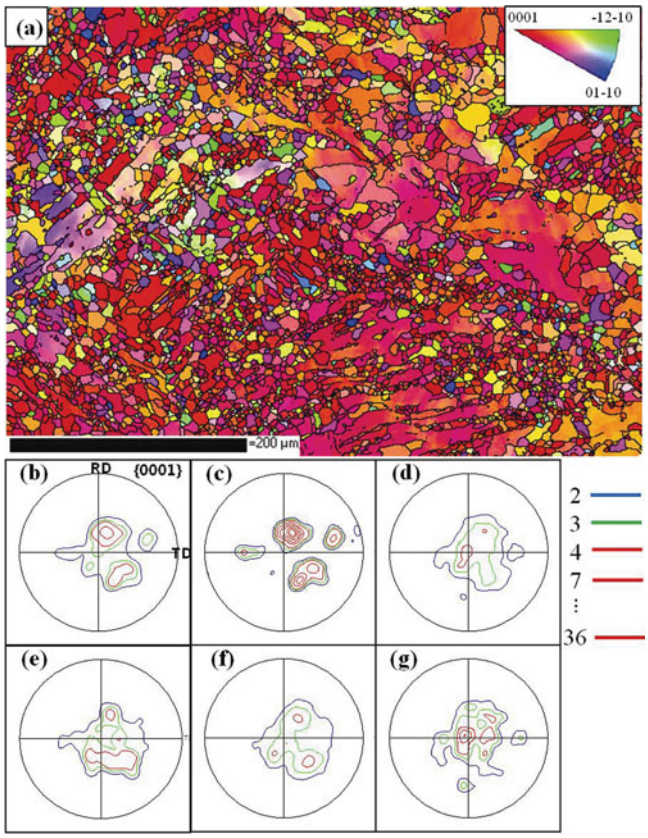

Figure 3. (**a**) Electron backscattered diffractometry orientation map and {0001} pole figures of a partially recrystallized sample for (**b**) overall area, (**c**) deformed grains (GOS $>$ 1.5°), (**d**) recrystallized grains (GOS $<$ 1.5°), (**e**) small recrystallized grains (GOS $<$ 1.5°; size $<$ 3.8 μm), (**f**) medium recrystallized grains (GOS $<$ 1.5°; 3.8 μm $<$ size $<$ 11.6 μm), and (**g**) large recrystallized grains (GOS $<$ 1.5°; size $>$ 11.6 μm).

over 90% of the sample was recrystallized. The average grain size of the recrystallized grains was 14.0 μm. Figures 4b–4d show pole figures for overall area, deformed grains (GOS $>$ 1.5°), and recrystallized grains (GOS $<$ 1.5°), respectively. As the area fraction of deformed grains was very small, the pole figures of the overall area and of the recrystallized grains are very similar. However, strong split basal texture was still observed in the deformed grains. It should be noted that the annealed texture was close to the basal texture and that the basal texture intensity of the grown grains was stronger than that of the smaller grains that occurred during early annealing (Figs. 3d, 3e). The statistical analysis of the evolution of recrystallization texture in cold-rolled AZ31 magnesium alloy sheet found that recrystallized grains were confirmed to have widely spread basal poles during nucleation but strong {0001} basal texture developed during the subsequent grain growth given by sufficient annealing.

Summary

In summary, the texture development in magnesium alloy sheets during rolling and annealing, which can influence the mechanical properties of the sheet, was observed by XRD and EBSD. The texture of cold-rolled sheets exhibits split peaks in RD; basal texture gradually strengthened with annealing time. To distinguish recrystallized grains from deformed grains in the EBSD orientation map, intra-grain misorientation was analyzed through GOS. From the statistical analysis of texture evolution, the recrystallized grains were found to show broadly spread basal poles during early annealing; after subsequent grain growth given by sufficient annealing, the recrystallized grains showed strong {0001} basal texture.

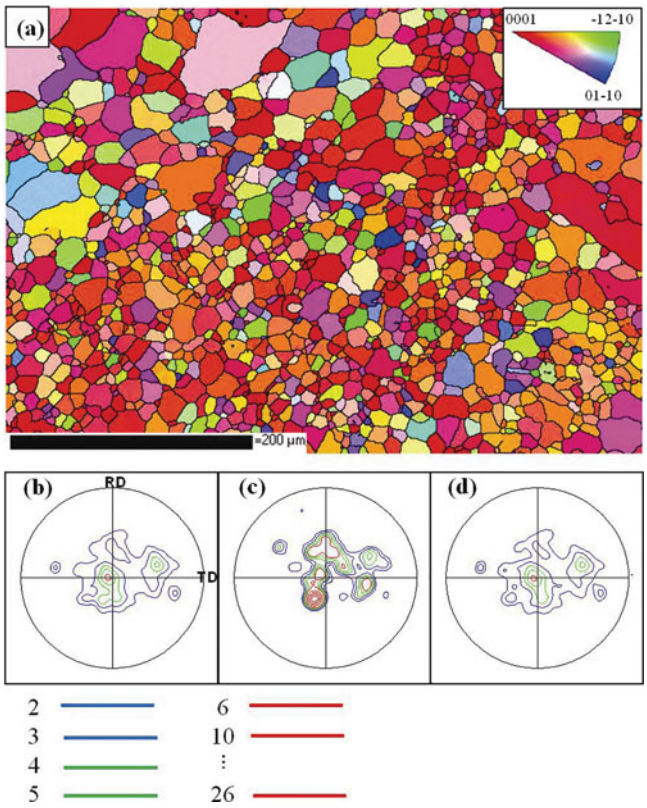

Figure 4. (**a**) Electron backscattered diffractometry orientation map and {0001} pole figures of an almost fully recrystallized sample for (**b**) overall area, (**c**) deformed grains (GOS $>$ 1.5°), and (**d**) recrystallized grains (GOS $<$ 1.5°).

Acknowledgments

This study was supported by National Research Foundation of Korea grant funded by the Ministry of Education, Science and Technology (2010-0018936).

References

Barnett, M.R., Nave, M.D. & Bettles, C.J. (2004). Deformation microstructures and textures of some cold rolled Mg alloys. *Mater Sci Eng A* **386**, 205–211.

Chino, Y. & Mabuchi, M. (2009). Enhanced stretch formability of Mg-Al-Zn alloy sheets rolled at high temperature (723 K). *Scr Mater* **60**, 446–450.

Easton, M., Beer, A., Barnett, M., Davies, C., Dunlop, G., Durandet, Y., Blacket, S., Hilditch, T. & Beggs, P. (2008). Magnesium alloy applications in automotive structures. *JOM* **60**, 57–62.

https://doi.org/10.1017/S1431927613012257 Published online by Cambridge University Press

Étienne, M., Mishra, R.K. & Jonas, J.J. (2010). Deformation structures and recrystallization in magnesium alloys. In *Magnesium Alloys—Design, Processing and Properties*, Czerwinski, F. (Ed.), pp. 21–42. Croatia: InTech.

Field, D.P. (1995). Quantification of partially recrystallization polycrystals using electron backscatter diffraction. *Mater Sci Eng* **A190**, 241–246.

Ha, S., Kim, S.-J., Hong, S., Yim, C.-D., Kim, D.-I., Suh, J., Oh, K.H. & Han, H.N. (2010). Improvement of ductility in magnesium alloy sheet using laser scanning treatment. *Mater Lett* **64**, 425–427.

Huang, X.S., Suzuki, K. & Saito, N. (2009). Textures and stretch formability of Mg-6Al-1Zn magnesium alloy sheets rolled at high temperaturers up to 793K. *Scr Mater* **60**, 651–654.

Kang, N.E., Yim, C.D., You, B.S. & Park, I.M. (2010). Fracture behavior of AZ31-xCa (x=0, 0.7, 2.0 wt.%) extrudes during compression. *Kor J Met Mater* **48**, 85–89.

Keshavarz, Z. & Barnett, M.R. (2006). EBSD analysis of deformation modes in Mg-3Al-1Zn. *Scr Mater* **55**, 915–918.

Kim, D.I., Oh, K.H. & Lee, H.-C. (2002). Statistical analysis on the development of recrystallization texture in IF steel. *Mater Sci Forum* **408–412**, 839–844.

Kim, D.I., Oh, K.H., Lee, H.-C. & Chang, Y.J. (2004). Characterization of crystallographic properties of SMC poly Si using electron backscattered diffraction. *J Microsc* **215**, 121–126.

Lee, B.H., Kim, S.M., Mehtedi, M.E., Evangelista, E. & Lee, C.S. (2010). Effect of stress state on the high temperature workability of AZ31 Mg alloy. *Met Mater Int* **16**, 197–203.

Mordike, B.L. & Ebert, T. (2001). Magnesium properties—applications—potential. *Mater Sci Eng* **A302**, 37–45.

Park, N.-J. & Han, S.-H. (2010). Effects of rolling temperature on the development of microstructure, texture, and mechanical properties in AZ31 magnesium alloy. *Kor J Met Mater* **48**(6), 498–505.

Pérez-Prado, M.T., del valle, J.A. & Ruano, O.A. (2004). Effect of sheet thickness on the microstructural evolution of an Mg AZ61 alloy during large strain hot rolling. *Scr Mater* **50**, 667–671.

Pérez-Prado, M.T. & Ruano, O.A. (2003). Texture evolution duting grain growth in annealed Mg AZ61 alloy. *Scr Mater* **48**, 59–64.

Styczynski, A., Hartig, C., Bohlen, J. & Letzig, D. (2004). Cold rolling textures in AZ31 wrought magnesium alloy. *Scr Mater* **50**, 943–947.

https://doi.org/10.1017/S1431927613012257 Published online by Cambridge University Press